Spectroscopic evidence of quantum Hall interlayer tunneling gap collapse caused by tilted magnetic field in a GaAs/AlGaAs triple quantum well

L. Fernandes dos Santos,[1] B. G. Barbosa,[1] G. M. Gusev,[2] J. Ludwig,[3,4] D. Smirnov,[3] A. K. Bakarov,[5,6] and Yu. A. Pusep[1]

[1]*Instituto de Fisica de São Carlos, Universidade de São Paulo, 13560-970 Sao Carlos, SP, Brazil*

[2]*Instituto de Física da Universidade de São Paulo, CP 66318 CEP 05315-970, São Paulo, SP, Brazil*

[3]*National High Magnetic Field Laboratory, Tallahassee, Florida 32312, USA*

[4]*Department of Physics, Florida State University, Tallahassee, Florida 32306, USA*

[5]*Institute of Semiconductor Physics, Novosibirsk 630090, Russia*

[6]*Novosibirsk State University, Novosibirsk, 630090, Russia*

(Received 5 November 2013; revised manuscript received 22 April 2014; published 9 May 2014)

Magnetophotoluminescence and magnetotransport were studied in a GaAs/AlGaAs triple quantum well. Oscillations of the photoluminescence intensity observed in tilted magnetic fields were found to correspond to the interlayer tunneling quantum Hall gap collapses detected in magnetoresistance measurements and predicted to occur in tilted magnetic fields. The obtained experimental data were shown to agree well with the theory developed for double quantum wells. This implies that the observed quantum Hall gap collapses are mostly caused by the tunneling between a pair of quantum wells. Our results reveal spectroscopic evidence of the quantum Hall gap collapses. Indications of interlayer correlation effects influencing a character of the inter-Landau-level gaps were found.

DOI: 10.1103/PhysRevB.89.195113 PACS number(s): 73.43.Lp, 73.43.Nq, 78.67.Pt

I. INTRODUCTION

Multicomponent electron systems formed in multiple-quantum-well (MQW) semiconductor heterostructures have been the subject of intense studies [1,2], resulting in discoveries of such striking phenomena as the collapse of the integer quantum Hall effect [3,4], spontaneous interlayer phase coherence [5–7], and excitonic Bose condensation [8–10]. An additional layer degree of freedom associated with the third dimension in a MQW system allows for controlling the competition between intrawell and interwell electron-electron correlations. Depending on the ratio d/l, where d is the interlayer separation and l is the magnetic length, different ground states can be realized in quantum Hall MQWs [11,12].

The correlation effects in quantum Hall (QH) multilayers have been mostly studied in bilayers using magnetotransport [13,14], inelastic scattering [15,16], and magnetophotoluminescence (magneto-PL) [17,18] measurements. It is worth mentioning that the effects of electron correlations were also observed in a high-mobility weakly coupled MQW embedded in a wide AlGaAs parabolic well where the quantum transition manifesting itself in a redistribution of the electron density over the quantum wells was found in Refs. [19–21]. An important result of electron correlations in MQW is the collapse of the QH tunneling gaps, which has been predicted to occur in coupled QH bilayers in tilted magnetic fields B in Ref. [22] and observed experimentally in Refs. [13,14]. This phenomenon relates to the angular-dependent magnetoresistance oscillations (AMRO) found in layered Fermi systems with a weakly corrugated cylindrical Fermi surface. The AMRO effect manifests itself as the resistance oscillatory changes in an angular trace of magnetoresistance and implies the interlayer tunneling rate vanishing at certain angles. Such oscillations were first observed in layered organic conductors [23] and explained as a result of semiclassical Fermi-surface topological effects [24]. The theory developed by Yamaji [24] implies coherent interlayer transport. Afterward, it was established that AMRO is essentially the same for both coherent and incoherent interlayer transport [25], and therefore, the existence of the three-dimensional Fermi surface suggested in Ref. [24] is not necessary. In quantum Hall multilayer electron systems the interlayer tunneling rate is responsible for corresponding quantum Hall tunneling gaps, which, according to AMRO, collapse at certain angles. An intuitive interpretation based on the Aharonov-Bohm effect suggests that the gap collapse results from destructive interference in the effective tunneling amplitude at particular angles of the magnetic field [26].

The interlayer coupling that leads to a finite tunneling gap is essential for the collapse of the QH tunneling gaps. Thus, similar to AMRO, the quantum Hall tunneling gap collapses may be observed in coupled MQW (superlattices). However, the collapsing of the tunneling gaps critically depends on the electron mobility, which is considerably lower in coupled MQWs than in coupled bilayers. It is for this reason that the collapsing of the tunneling gap has not been observed in MQWs to date. On the other hand, it is still an open question whether the QH gap collapse in MQWs is dominated by the tunneling between a pair of nearest-neighbor quantum wells or if the next-nearest-neighbor quantum well also contributes. High-mobility triple quantum wells (TQWs) were reported in Refs. [27,28], where the integer QH effect and field-induced trilayer-to-bilayer transition were observed. In addition, the emergent and reentrant fractional QH effect in a tilted magnetic field [29] and microwave-induced effects [30] were also recently found. Such high-mobility TQW presents a good candidate to explore the influence of several quantum wells on the quantum Hall tunneling gap collapse.

II. EXPERIMENT

Magneto-optical spectroscopy probes the energy distribution of the electron density of states and therefore provides important information about electron correlations, complementary to magnetotransport measurements. In this work we report on the data obtained by magnetotransport and magneto-PL of a highly doped GaAs TQW separated by

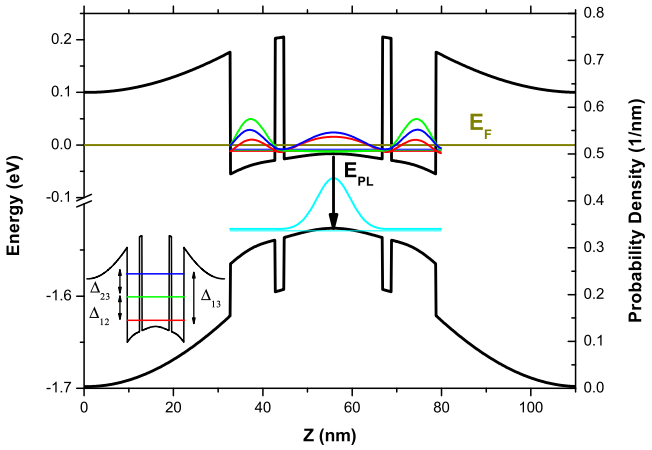

FIG. 1. (Color online) Zero-field electronic energy structure (black line) and the charge-density profiles (colored lines) self-consistently calculated for the GaAs/AlGaAs triple-quantum-well structure with the total electron sheet density $n_s = 7 \times 10^{11}$ cm^{-2}. The inset shows the schematic of the size-quantized states in the conduction band with interlayer tunneling gaps Δ_{12}, Δ_{23}, and Δ_{13}.

$Al_xGa_{1-x}As$ barriers, focusing on the effects of the tilted magnetic field B. It ought to be pointed out that the magneto-PL in QH TQWs remains largely unexplored. As demonstrated in Ref. [22] for coupled QH bilayers, a parallel magnetic field component results in the collapse of the quantum Hall tunneling gap between symmetric and antisymmetric electron states. As a consequence, QH states associated with the tunneling gap disappear [13,14]. This happens at certain critical magnetic fields determined by the zeros of the magnetic-field-dependent interlayer tunneling gap Δ_ν, where ν is the filling factor corresponding to the tunneling gap [22]:

$$\Delta_\nu = \Delta_0 e^{-\alpha^2} L_\nu(2\alpha^2), \tag{1}$$

where Δ_0 is the zero-field gap, $\alpha = B_\parallel d / B_\perp l_\perp$ with d and $l_\perp = (\hbar/eB_\perp)^{1/2}$ are defined as the interlayer distance and the perpendicular magnetic length, respectively, $B_\parallel$ and $B_\perp$ are magnetic field components parallel and perpendicular to the plane of the sample, and L_ν is a Laguerre polynomial.

In the TQW considered here, the interlayer coupling results in the formation of three subbands separated by interlayer tunneling gaps Δ_{12}, Δ_{23}, and Δ_{13}, shown in the inset of Fig. 1. The collapse of the tunneling gap leads to a modulation of the conduction band density of states and, as a consequence, to a corresponding change in PL intensity. We found oscillations in the PL intensity with the magnetic field which correlate with the collapsing tunneling gaps Δ_{12} and Δ_{23} observed in magnetoresistance measurements. This is the spectroscopic observation of the tunneling gap collapses due to quantum interference in QH multilayers.

The TQW studied here consists of a 22-nm-thick GaAs central well and two 10-nm-thick lateral wells each separated by 2-nm-thick $Al_{0.3}Ga_{0.7}As$ barriers. The samples are symmetrically δ doped, and we find that the total electron sheet density $n_s = 7 \times 10^{11}$ cm^{-2} and the low-temperature mobility $\mu = 4 \times 10^5$ cm^2/V s. Samples for transport measurements were patterned into 200-μm-wide Hall bars with the voltage probes 500 μm apart. The layers were shunted by In Ohmic contacts. The magnetotransport measurements were carried out at $T = 50$ mK in a dilution refrigerator using a conventional ac lock-in technique with a bias current in the range of 0.01–0.1 μA. Four-terminal resistance R_{xx} was measured in magnetic fields up to 15 T, varying the angle of the magnetic field from $\theta = 0^\circ$ to 80°, where θ is measured with respect to the surface normal. The circularly polarized PL was measured at $T \simeq 300$ mK with magnetic fields up to 18 T applied perpendicular to the sample surface $\theta = 0^\circ$ or $\theta = 55^\circ$. A single 365-μm-diameter optical fiber delivers the laser excitation (wave length $\lambda = 532$ nm, and power density $W \approx 1$ mW/cm^2) to the sample in a ^{3}He cryostat. In order to perform circularly polarized measurements a linear polarizer and a quarter-wave plate are installed in front of the sample. The σ^+ and σ^- circularly polarized PL components are selected by reversing the polarity of the magnetic field. The σ^+ component is related to the transition between the electron spin state $m_j = -1/2$ and the heavy-hole state with $m_j = -3/2$, while the heavy-hole state with $m_j = +3/2$ and the electron spin state $m_j = +1/2$ are responsible for the emission of the σ^- component.

III. RESULTS AND DISCUSSION

Figure 1 shows the zero-field band structure and the charge distribution profiles proportional to the probability density calculated using a self-consistent Schrödinger-Poisson solver [31]. According to the calculations, the electrons occupy the three lowest closely spaced size-quantized subbands distributed over an energy interval of a few meV. The resultant intersubband gaps are $\Delta_{12} \approx 1.8$ meV and $\Delta_{23} \approx 2.0$ meV. The experimentally determined interlevel gaps $\Delta_{12} = 1.4$ meV and $\Delta_{23} \approx 3.9$ meV can be found in Ref. [30]. In the valence band, photoexcited holes accumulate on the lowest level confined at the center of the structure. Thus, the PL intensity mostly measures the radiative recombination between the electrons and holes in the central quantum well.

The plot of the σ^- polarized PL intensity as a function of the perpendicular component of the magnetic field $B_\perp = B\cos\theta$ measured at $\theta = 55^\circ$ is depicted in Fig. 2, showing two distinct lines. The low-energy line is likely due to the exciton bound to a neutral donor (DX center) [32–34], while the more intense high-energy line relates to the direct recombination between the states confined in the conduction and valence bands. A relatively large broadening of the observed PL lines (about 2 meV) is mostly determined by the broadening of the electron levels in the valence band. Contrary to the magnetotransport measurements where the high mobility of the conduction band electrons allows for the clear observation of individual QH states, separate emissions from individual electron subbands formed in the conduction band are not distinguished. Nevertheless, as demonstrated below, a modulation of the conduction band density of states formed by three close electron levels, driven by the tunneling gap collapse, is definitely detected. Corresponding oscillations of the PL intensity are observed in the high magnetic fields at tilted angles. Figure 2 shows the PL intensity oscillations for σ^- as a function of magnetic field for $\theta = 55^\circ$. Similar PL intensity oscillations were found for σ^+ polarized PL intensity. It is worth mentioning that the intensity of the PL line attributed to the excitons bound to the DX center shows magnetic-field-induced intensity

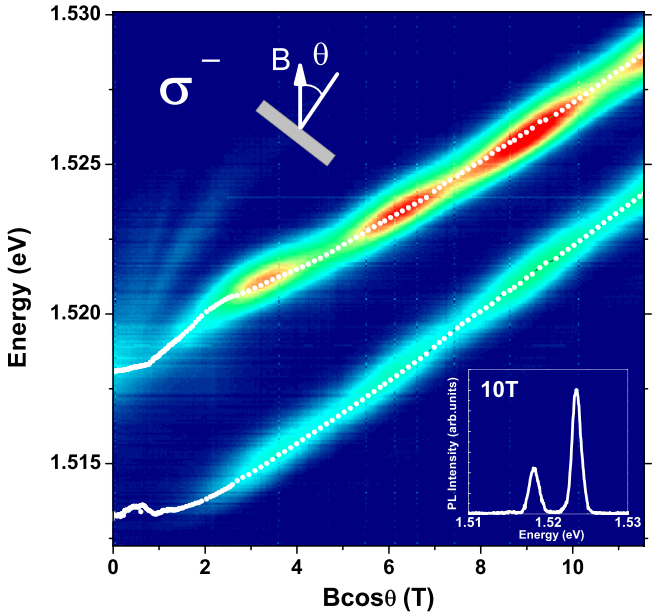

FIG. 2. (Color online) σ^- polarized PL intensity measured at the tilt angle $\theta = 55^\circ$ in the GaAs/AlGaAs triple quantum well as a function of the perpendicular component of the magnetic field at the temperature $T = 300$ mK. White dots indicate the PL peak positions. The inset shows representative PL spectra measured at a magnetic field of 0 T and $\theta = 0^\circ$ (thin yellow line) and 10 T and $\theta = 55^\circ$ (thick white line).

modulations similar to the modulation of the PL line caused by the interband recombination, albeit weakened. We suppose that this happens because some electrons occupying the Landau levels in the conduction band recombine with the holes in the valence band through intermediate-energy levels corresponding to the excitons bound to DX centers. As a consequence, both the direct recombination of the excitons bound to DX centers and the interband recombination of the electrons located on the Landau levels mediated by DX centers contribute to the PL line attributed to the emission caused by DX centers. In such cases changes in the intensity of the interband recombination will also result in corresponding changes in the intensity of the PL line due to DX centers. In addition, the formation of the Landau levels associated with the conduction miniband states is clearly seen in the weak magnetic field range.

The Landau-level fan chart together with the Fermi level as a function of the magnetic field calculated for the TQW studied here are depicted in Fig. 3. The energy structure of the TQW is established by the Landau levels separated by the tunneling, spin-split, and cyclotron gaps. The only tunneling gaps relevant to the present study depicted in Fig. 3 are Δ_{12}, Δ_{23}, and Δ_{13}. The effective g factor used in the calculations was determined by analysis of the Landau-level crossing diagram [14,35,36]. In the TQW studied here the Landau-level crossing observed in the perpendicular magnetic field yields an effective g factor of 13. At particular tilt angles determined by Eq. (1), the quantum interference causes the collapses of the tunneling gaps, which correspond to the filling factors $\nu = 1,2,4,5,7,9, \ldots$ Some of these collapses were indeed found in magnetotransport experiments.

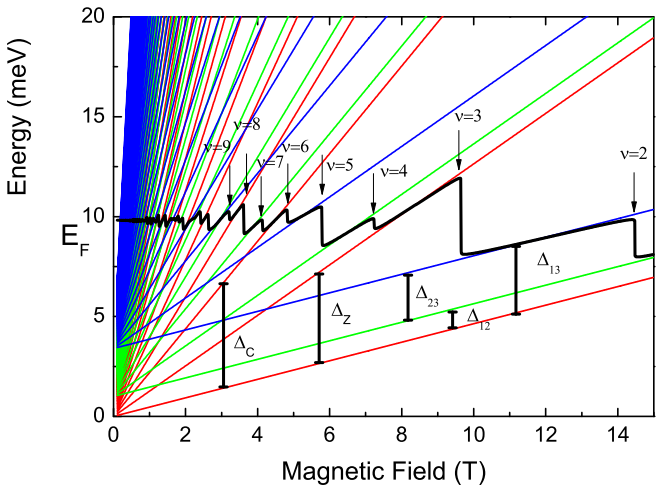

FIG. 3. (Color online) Landau-level energy structure of the GaAs/AlGaAs triple quantum well. The position of the Fermi level calculated with the total electron sheet density $n_s = 7 \times 10^{11}$ cm^{-2} is shown by the black line. The numbers depict corresponding filling factors. The related cyclotron Δ_c, Zeeman Δ_Z, and interlayer tunneling gaps Δ_{12}, Δ_{23}, and Δ_{13} are indicated by vertical bars.

Magnetoresistance measured on the same sample as a function of the tilt angle is demonstrated in Fig. 4(a). The contrast of the plot is chosen in order to show more clearly the observed quantum Hall gap collapses; therefore, it does not demonstrates absolute resistance values. In order to directly compare to the PL spectra, the magnetoresistance traces measured at the perpendicular magnetic field and at the tilt angle $\theta = 55^\circ$ are shown in Fig. 4(b). At certain titled angles of the magnetic field, the collapse of the QH tunneling gap appears as a finite resistance where R_{xx} goes to zero in the perpendicular configuration, $\theta = 0^\circ$. These collapses are clearly observed in Figs. 4(a) and 4(b) at filling factors $\nu = 4,5,8,9$. According to the Landau-level fan chart shown in Fig. 3, the gaps corresponding to the filling factors $\nu = 4,5$ and $\nu = 9$ are due to the interlayer tunneling (Δ_{12}, Δ_{23} and Δ_{12}, respectively), while the one at $\nu = 8$ is caused by the Zeeman gap. We suppose that the gap observed at the filling factor $\nu = 8$ is due to interlayer tunneling, which changed its character due to electron-electron interaction. As demonstrated in Refs. [3,17,20,28,37–42], the electron correlations in MQWs lead to the formation of a collective ground state, like a charge-density wave, which manifests itself in a corresponding redistribution of the electron density over the quantum wells. Such changes in the local electron density may modify the character of the gaps in the range of the magnetic field where the interaction energy is comparable to the Landau-level separation. Thus, in the range of magnetic fields where the separation of the Landau levels is small, the gap at the filling factor $\nu = 8$ turns out to be the tunneling gap, instead of the spin-split gap predicted by single-particle calculations. The large effective g factor obtained in the structure studied here also indicates the importance of electron-electron correlations. The QH gap collapses calculated according to Eq. (1) at the tilt angle $\theta = 55^\circ$ and the interlayer distance $d = 6$ nm are indicated by arrows in Fig. 4(c). As a result, the theory presented in [22] is found be able to reproduce the essential features of

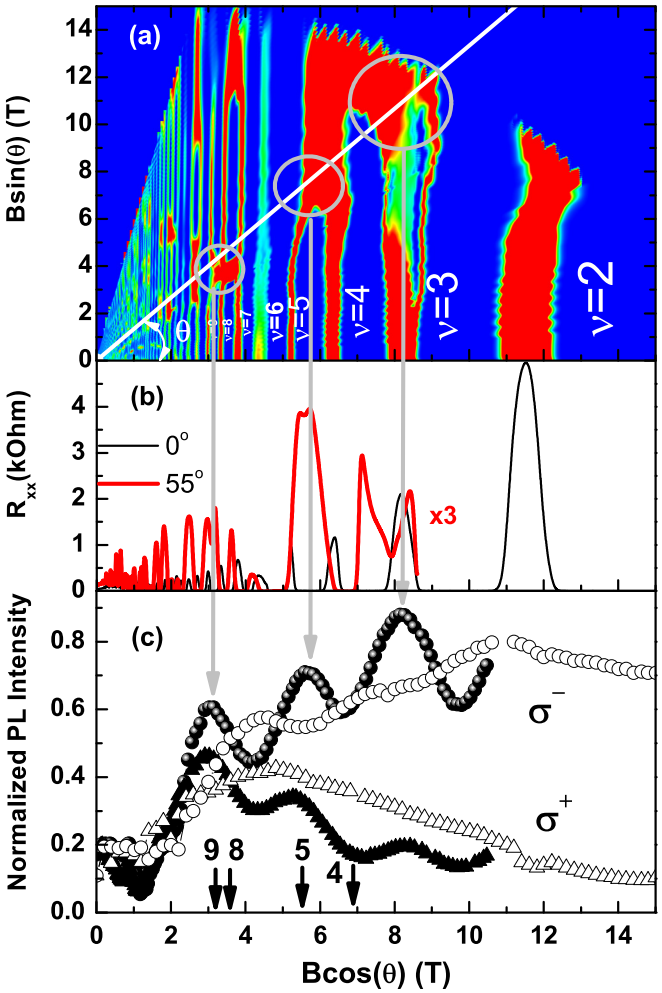

FIG. 4. (Color online) (a) Plot of the magnetoresistance measured at the temperature $T = 50$ mK in the GaAs/AlGaAs triple quantum well as a function of the tilting angle. The white line corresponds to the tilting angle $\theta = 55^\circ$. Open gray circles indicate the collapses observed in both the magnetoresistance and photoluminescence measurements. (b) Magnetoresistance traces measured at tilt angles $\theta = 0^\circ$ (black line) and $\theta = 55^\circ$ (red line). (c) σ^+ (triangles) and σ^- (circles) normalized photoluminescence intensities measured at $T = 300$ mK in the GaAs/AlGaAs triple quantum well as a function of the perpendicular magnetic field component at $\theta = 0^\circ$ (open symbols) and at $\theta = 55^\circ$ (solid symbols). The positions of the intersubband quantum Hall gap collapses calculated according to Eq. (1) for the corresponding filling factors are shown by arrows.

the magnetoresistance measured in tilted magnetic fields in a TQW.

Normalized σ^+ and σ^- PL intensities measured at $\theta = 0^\circ$ and $\theta = 55^\circ$ are also shown in Fig. 4(c). In the perpendicular magnetic field $\theta = 0^\circ$, weak maxima were observed in the σ^- polarized PL intensity. They are associated with the corresponding insulating integer quantum Hall states, at which weaker screening results in a PL intensity that is higher than the metallic quantum Hall states [43,44]. No such oscillations were found in the σ^+ polarized PL intensity, which is likely due to the weaker σ^+ intensity. Three distinct peaks were found in both polarizations when the magnetic field was tilted to $\theta = 55^\circ$. Independent of polarization these peaks are observed at the same values of the magnetic field. Therefore, they cannot be attributed to the magnetic-field-induced variations in the occupied density of states of the Landau levels nearest the Fermi energy as detected in Ref. [45]. We assign the PL intensity maxima found in the tilted magnetic field to the collapses of the tunneling gaps shown in the magnetoresistance plot by open gray circles. The collapses of the tunneling gaps result in the increasing density of the electron states in the conduction band and, as a consequence, in the increasing PL intensity. The first peak takes place at the magnetic field corresponding to the superposition of the collapses of the gaps associated with $\nu = 8$, $\nu = 9$ (which are resolved neither spectroscopically nor by magnetotransport measurements) and $\nu = 11$, while the second and third PL peaks are related to the collapses of the tunneling gaps at $\nu = 5$ and $\nu = 4$. Our results indicate that the collapses take place over a fairly large interval of the magnetic fields around the tunneling gap.

IV. CONCLUSION

The collapsing quantum Hall tunneling gaps caused by tilted magnetic field were found in GaAs/AlGaAs triple quantum wells independently by magnetotransport and magnetophotoluminescence measurements. The inconsistency in the character of the quantum Hall gap found experimentally and determined by single-particle calculations is explained by interlayer electron correlations, which cause a redistribution of the electrons over the quantum wells, thus changing the character of the gaps. The theory developed for double quantum wells in Ref. [22] reproduces reasonably well the results obtained in the triple quantum wells. This means that the fundamental contribution to the observed quantum Hall gap collapses is due to the tunneling between a pair of nearest-neighbor quantum wells.

ACKNOWLEDGMENTS

Financial support from the Brazilian agencies FAPESP and CNPq is gratefully acknowledged. Part of this work was performed at NHMFL in Tallahassee, Florida, which is supported by National Science Foundation Cooperative Agreement No. DMR-1157490 and by the state of Florida.

[1] J. P. Eisenstein, in *Perspectives in Quantum Hall Effects*, edited by S. Das Sarma and A. Pinczuk (Wiley, New York, 1997), Chap. 2, p. 37; S. M. Girvin and A. H. MacDonald, *ibid.*, Chap. 5, p. 161.
[2] S. M. Girvin, Phys. Today **53**(6), 39 (2000).
[3] G. S. Boebinger, H. W. Jiang, L. N. Pfeiffer, and K. W. West, Phys. Rev. Lett. **64**, 1793 (1990).
[4] A. H. MacDonald, P. M. Platzman, and G. S. Boebinger, Phys. Rev. Lett. **65**, 775 (1990).
[5] J. P. Eisenstein, L. N. Pfeiffer, and K. W. West, Phys. Rev. Lett. **69**, 3804 (1992).
[6] I. B. Spielman, J. P. Eisenstein, L. N. Pfeiffer, and K. W. West, Phys. Rev. Lett. **84**, 5808 (2000).
[7] J. Eisenstein, Solid State Commun. **127**, 123 (2003).

[8] M. Kellogg, J. P. Eisenstein, L. N. Pfeiffer, and K. W. West, Phys. Rev. Lett. **93**, 036801 (2004).
[9] E. Tutuc, M. Shayegan, and D. A. Huse, Phys. Rev. Lett. **93**, 036802 (2004).
[10] J. Eisenstein, Science **305**, 950 (2004).
[11] C. B. Hanna, J. C. Díaz-Vélez, and A. H. MacDonald, Phys. Rev. B **65**, 115323 (2002).
[12] M. R. Peterson and S. Das Sarma, Phys. Rev. B **81**, 165304 (2010).
[13] G. M. Gusev, A. K. Bakarov, T. E. Lamas, and J. C. Portal, Phys. Rev. Lett. **99**, 126804 (2007).
[14] G. M. Gusev, C. A. Duarte, T. E. Lamas, A. K. Bakarov, and J. C. Portal, Phys. Rev. B **78**, 155320 (2008).
[15] V. Pellegrini, S. Luin, B. Karmakar, A. Pinczuk, B. S. Dennis, L. N. Pfeiffer, and K. W. West, J. Appl. Phys. **101**, 081718 (2007).
[16] B. Karmakar, V. Pellegrini, A. Pinczuk, L. N. Pfeiffer, and K. W. West, Int. J. Mod. Phys. B **23**, 2607 (2009).
[17] Y. A. Pusep, L. F. dos Santos, G. M. Gusev, D. Smirnov, and A. K. Bakarov, Phys. Rev. Lett. **109**, 046802 (2012).
[18] I. Aliaj, V. Pellegrini, A. Gamucci, B. Karmakar, A. Pinczuk, L. N. Pfeiffer, and K. W. West, Phys. Rev. B **87**, 161303(R) (2013).
[19] G. M. Gusev, Yu. A. Pusep, A. K. Bakarov, A. I. Toropov, and J. C. Portal, Phys. Rev. B **81**, 165302 (2010).
[20] L. Fernandes dos Santos, Yu. A. Pusep, G. M. Gusev, A. K. Bakarov, and A. I. Toropov, Europhysics Lett. **97**, 17010 (2012).
[21] Yu. A. Pusep, L. Fernandes dos Santos, D. Smirnov, A. K. Bakarov, and A. I. Toropov, Phys. Rev. B **85**, 045302 (2012).
[22] J. Hu and A. H. MacDonald, Phys. Rev. B **46**, 12554 (1992).
[23] M. V. Kartsovnik, P. A. Kononovich, V. N. Laukhin, and I. F. Shchegolev, JETP Lett. **48**, 541 (1988).
[24] K. Yamaji, J. Phys. Soc. Jpn. **58**, 1520 (1989).
[25] R. H. McKenzie and P. Moses, Phys. Rev. Lett. **81**, 4492 (1998).
[26] V. M. Yakovenko and B. K. Cooper, Phys. E (Amsterdam, Neth.) **34**, 128 (2006).
[27] J. Jo, Y. W. Suen, L. W. Engel, M. B. Santos, and M. Shayegan, Phys. Rev. B **46**, 9776 (1992).
[28] S. P. Shukla, Y. W. Suen, and M. Shayegan, Phys. Rev. Lett. **81**, 693 (1998).
[29] G. M. Gusev, S. Wiedmann, O. E. Raichev, A. K. Bakarov, and J. C. Portal, Phys. Rev. B **80**, 161302(R) (2009).
[30] S. Wiedmann, N. C. Mamani, G. M. Gusev, O. E. Raichev, A. K. Bakarov, and J. C. Portal, Phys. Rev. B **80**, 245306 (2009).
[31] I.-H. Tan, G. L. Snider, L. D. Chang, and E. L. Hu, J. Appl. Phys. **68**, 4071 (1990).
[32] L. Pavesi and M. Guzzi, J. Appl. Phys. **75**, 4779 (1994).
[33] G. Finkelstein, H. Shtrikman, and I. Bar-Joseph, Phys. Rev. B **53**, 12593 (1996).
[34] O. V. Volkov, V. E. Zhitomirskii, I. V. Kukushkin, V. E. Bisti, K. von Klitzing, and K. Eberl, JETP Lett. **66**, 766 (1997).
[35] C. Ellenberger, B. Simovič, R. Leturcq, T. Ihn, S. E. Ulloa, K. Ensslin, D. C. Driscoll, and A. C. Gossard, Phys. Rev. B **74**, 195313 (2006).
[36] C. A. Duarte, G. M. Gusev, A. A. Quivy, T. E. Lamas, A. K. Bakarov, and J. C. Portal, Phys. Rev. B **76**, 075346 (2007).
[37] P. P. Ruden and Z. Wu, Appl. Phys. Lett. **59**, 2165 (1991).
[38] A. F. M. Anwar and M. M. Jahan, Phys. Rev. B **50**, 10864 (1994).
[39] L. Zheng, M. W. Ortalano, and S. Das Sarma, Phys. Rev. B **55**, 4506 (1997).
[40] S. J. Papadakis, J. P. Lu, M. Shayegan, S. R. Parihar, and S. A. Lyon, Phys. Rev. B **55**, 9294 (1997).
[41] H. C. Manoharan, Y. W. Suen, T. S. Lay, M. B. Santos, and M. Shayegan, Phys. Rev. Lett. **79**, 2722 (1997).
[42] V. V. Solovyev, S. Schmult, W. Dietsche, and I. V. Kukushkin, Phys. Rev. B **80**, 241310(R) (2009).
[43] B. B. Goldberg, D. Heiman, A. Pinczuk, L. Pfeiffer, and K. West, Phys. Rev. Lett. **65**, 641 (1990).
[44] K. Meimberg, M. Potemski, P. Hawrylak, Y. H. Zhang, and K. Ploog, Phys. Rev. B **55**, 7685 (1997).
[45] L. Fernandes dos Santos, Yu. A. Pusep, L. Villegas-Lelovsky, V. Lopez-Richard, G. E. Marques, G. M. Gusev, D. Smirnov, and A. K. Bakarov, Phys. Rev. B **86**, 125415 (2012).